

THE COMPLEX OF PANT DECOMPOSITIONS OF A SURFACE

SILVIA BENVENUTI AND RICCARDO PIERGALLINI

ABSTRACT. We exhibit a set of edges (*moves*) and 2-cells (*relations*) making the complex of pant decompositions on a surface a simply connected complex. Our construction, unlike the previous ones, keeps the arguments concerning the structural transformations independent from those deriving from the action of the mapping class group. The moves and the relations turn out to be supported in subsurfaces with $3g - 3 + n = 1, 2$ (where g is the genus and n is the number of boundary components), illustrating in this way the so called Grothendieck principle.

CONTENTS

1. Introduction	1
2. First definitions and main tools	4
3. The combinatorial structures of pant decompositions	5
3.1. Reducing the number of boundary components	8
3.2. Dealing with the closed case	15
3.3. The decorated combinatorial structures	18
4. The complex of pant decompositions	19
4.1. The decorated pant decompositions	19
4.2. Back to pant decompositions	25
References	26

1. INTRODUCTION

Let $\Sigma = \Sigma_{g,n}$ be a connected, compact, oriented surface of genus g with n boundary components ($g, n \geq 0$). In order to describe an algebraic or geometric object $\tau(\Sigma)$, it is often convenient to represent Σ as the result of gluing together several simple pieces, which should be surfaces with boundary.

This happens for example in the study of the mapping class group $\mathcal{M}(\Sigma) = \mathcal{M}_{g,n}$ (whose presentation may be obtained starting from those of the mapping class group of some simple subsurfaces, as proved in [4]), in the pantwise construction of hyperbolic structures (Fenchel-Nielsen construction) and in the construction of modular functors (defined by gluing the vector spaces associated to simpler subsurfaces, provided they satisfy some *gluing axiom*).

Depending on the situation, it is convenient to choose the building blocks for our surfaces from different *Lego boxes*: one may choose, for example, a big Lego box (the *grande boîte* in [9]), whose pieces are all the spheres with any number of boundary components, or maybe a smaller Lego box, containing only spheres with at most three boundary components. In many cases, a *cheap* Lego box, made of identical pieces (namely spheres with three boundary components or hexagons) may be sufficient.

1991 *Mathematics Subject Classification*. Primary 57M50; Secondary 57M20, 30F60.

Key words and phrases. Pant decomposition complex, mapping class group, complex of curves.

No matter which box one chooses, it is evident that each surface admits an infinite number of different decompositions with pieces out of that box (see for instance Figure 1).

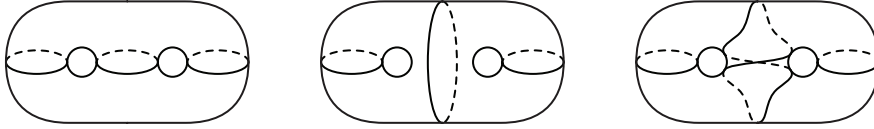


FIGURE 1. Three different pant decompositions of $\Sigma_{2,0}$.

Thus, if one wants to describe an object $\tau(\Sigma)$ using a decomposition d of Σ (i.e. computing $\tau(\Sigma)$ as a $\tau(\Sigma, d)$), in order for this object to be well defined it is necessary to construct canonical isomorphisms between the objects computed starting from different decompositions, i.e. to construct isomorphisms

$$f : \tau(\Sigma, d_1) \rightarrow \tau(\Sigma, d_2),$$

where d_1 and d_2 are any two different decompositions of Σ .

For instance, coming back to the cases mentioned before: while studying the mapping class group it turns out that different “slicing” of Σ produce different presentations for $\mathcal{M}(\Sigma)$, and we look for a procedure to get any presentation from any other; while constructing hyperbolic structures, different pant decompositions lead to the description of different charts of the atlas of the Teichmüller space of Σ , and we look for the change of chart; while building a modular functor, different ways of sewing Σ result in different bases for the vector space associated to Σ , and we need to write down the matrices giving the change of basis (*duality matrices* in [16]).

Therefore, once the Lego box is fixed, we have to describe the set of all the decompositions of a surface into pieces from that Lego box, considered up to isotopy, and the set of all the transformations between different (non-isotopic) decompositions. More precisely, our aim is to exhibit:

- elementary moves*, such that we can go from a given decomposition to any other through a sequence of these moves;
- defining relations*, describing when a sequence of elementary moves applied to a decomposition yields the same decomposition.

Following the philosophy introduced by Hatcher and Thurston in their pioneering paper [11], such problem can be reformulated as follows: we consider all the decompositions of the surface $\Sigma = \Sigma_{g,n}$ up to isotopy, as the vertices of a 2-dimensional CW complex $\mathcal{R}(\Sigma) = \mathcal{R}_{g,n}$; then we put an edge between two vertices if the corresponding decompositions are related by one of our candidate *moves*, and we cup off a loop with a 2-cell if the corresponding sequence of moves is one of our candidate *relations*. Hence we are reduced to check that $\mathcal{R}_{g,n}$ is simply connected. Indeed, this complex is connected if and only if the set of our candidates moves is complete. Moreover, it is simply connected if and only if any relation between elementary moves follows from the ones we have cupped off. Actually in [11] the focus is on the *cut system complex* $\mathcal{C}(\Sigma)$, but in the appendix the authors suggest that the same program could be carried over to the case of pant decompositions.

The *pant decomposition complex* $\mathcal{R}_{g,n}$ was studied in [16] by Moore and Seiberg. Unfortunately, their proof of the connectedness and simply connectedness of the so built complex contains some serious gaps. In particular, it is based on the knowledge of an explicit presentation for the mapping class groups $\mathcal{M}_{g,n}$, which was then unknown. Indeed, at the moment they were writing (1989), the only known finite presentations were those of the modular groups $\mathcal{M}_{0,n}$ and $\mathcal{M}_{g,0}$.

The mapping class group of the surface we are examining enters the playground since the elements of this group act as transformations on the set of the decompositions of Σ : for instance, the decomposition shown in the right hand picture of Figure 1 is obtained from the one in the center by a Dehn twist along the dotted curve. Anyway, not all transformations between decompositions are elements of the mapping class group: for instance, the decomposition shown in the left hand picture of Figure 1 cannot be transformed into the center one (nor into the right one) by any homeomorphism of Σ . Therefore, the set of transformations between different decompositions of the surface Σ contains a core, that is the mapping class group $\mathcal{M}(\Sigma)$, and something additional: the idea in [16] is to get rid of this “extra part” and eventually come to the study of $\mathcal{M}(\Sigma)$, which is what Moore and Seiberg could not carry out.

More recently, this problem has been overcome by using the Cerf theoretic techniques introduced in [11], either directly [6, 10] or passing through a projection on the cut systems complex [2].

In this paper, we come back to the original Moore and Seiberg’s approach and fill in the gaps, exploiting the presentations of the mapping class groups that we have at present.

Indeed, in [8], Gervais provides a presentation of $\mathcal{M}_{g,n}$, in terms of Dehn twists. Another presentation, as quotients of Artin groups, is described by Matsumoto in [14] for $\mathcal{M}_{g,1}$ and then generalized to the case of $\mathcal{M}_{g,n}$ by Labruère and Paris in [12].

A general machinery for getting presentations of the mapping class groups in any preferred “style” (for example in terms of Dehn twists or as quotients of Artin groups) is given in [4]. The procedure introduced in that paper takes as input the well known presentations for the *sporadic surfaces* ($\Sigma_{0,4}$, $\Sigma_{1,1}$, $\Sigma_{0,5}$ and $\Sigma_{1,2}$) according to some “style” and returns a presentation in the same “style” for every $\Sigma_{g,n}$. Such flexibility makes this last approach suitable for obtaining different descriptions of the complex $\mathcal{R}_{g,n}$ we may need in different contexts.

The paper is organized as follows. Section 2 contains the first definitions and the main tools. The construction of the complex $\mathcal{R}_{g,n}$ is subdivided into two independent steps. Given a surface $\Sigma_{g,n}$, in Section 3 we consider a 2-dimensional, finite, simply connected CW complex $\mathcal{S}_{g,n}$, whose vertices are in one-to-one correspondence with the *combinatorial structures* of pant decompositions of $\Sigma_{g,n}$, i.e. with the $\mathcal{M}_{g,n}$ -equivalence classes of such decompositions. Then, in Section 4, by using a presentation of $\mathcal{M}_{g,n}$, we construct an infinite simply connected complex codifying all the pant decompositions on $\Sigma_{g,n}$ and the transformations between them, that is the desired $\mathcal{R}_{g,n}$.

When we started thinking of this Lego-Teichmüller game, our aim was to understand something new about a Grothendieck conjecture on the subject (see [9]). In our context this conjecture can be expressed, roughly speaking, as follows. Take the family of all the complexes $\mathcal{R}_{g,n}$ and stack them in levels, putting at level k all the $\mathcal{R}_{g,n}$ with $3g - 3 + n = k$. Then, to describe the whole tower of complexes, it is sufficient to describe its first and second floor, i.e. the complexes with $3g - 3 + n = 1, 2$, that are precisely the ones of the sporadic surfaces $\Sigma_{0,4}$, $\Sigma_{1,1}$, $\Sigma_{0,5}$ and $\Sigma_{1,2}$.

It is worth noticing that we obtained this Grothendieck principle for the mapping class groups as a byproduct, in [4]. Namely, we proved that the generators and the relations which are needed to present the mapping class group of any surface are supported in subsurfaces living at the first and second Grothendieck floor. Combining this result with the new ones described in the present paper, we are now able to prove the Grothendieck conjecture in the above stated form.

2. FIRST DEFINITIONS AND MAIN TOOLS

Let $\Sigma = \Sigma_{g,n}$ be a connected, compact, oriented surface, of genus g with n boundary components. A *pant decomposition* of Σ is a decomposition of the surface into a finite number of pants, determined by a collection of disjoint simple closed curves in the interior of Σ . We recall that a *pant* is a closed disk with two smaller open disks removed, i.e. the surface $\Sigma_{0,3}$. As usual, the family of curves and therefore the induced pant decomposition are always considered up to isotopy.

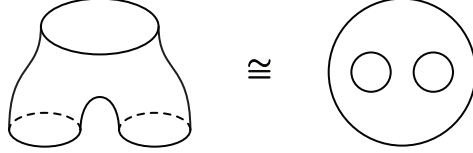


FIGURE 2. A pant.

More precisely, let $\alpha = \{\alpha_1, \dots, \alpha_k\}$ be a collection of pairwise disjoint closed loops on Σ . We denote by Σ_α the natural compactification of $\Sigma - \cup\{\alpha_i\}_{i=1,\dots,k}$ (obtained compactifying each component by the addition of three boundary curves), and by $\rho_\alpha : \Sigma_\alpha \rightarrow \Sigma$ the continuous map induced by the inclusion of $\Sigma - \cup\{\alpha_i\}_{i=1,\dots,k}$ into Σ .

Definition 1. We say that the family $\alpha = \{\alpha_1, \dots, \alpha_k\}$ determines a *pant decomposition* of Σ if each component of Σ_α is a pant, or equivalently if $\Sigma - \cup\{\alpha_i\}_{i=1,\dots,k}$ consists of h components, each of which is homeomorphic to the interior of a pant.

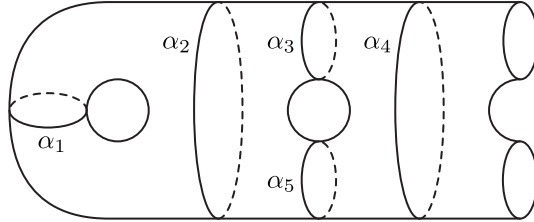


FIGURE 3. A pant decomposition.

It can be easily shown that $\Sigma_{g,n}$ admits a pant decomposition provided

$$(g, n) \notin \{(0, 0), (0, 1), (0, 2), (1, 0)\}.$$

Moreover, the integers k and h are uniquely determined, and they are given by

$$k = 3g - 3 + n \quad \text{and} \quad h = 2g - 2 + n = -\chi(\Sigma),$$

where $\chi(\Sigma)$ is the Euler characteristic of the surface Σ .

Let N be a connected component of Σ_α (notations as above). We say that a boundary curve γ of N is an *exterior boundary curve* if $\rho_\alpha(\gamma)$ is a boundary component of Σ . For each curve α_i in the family α there are two distinct boundary curves γ, γ' in Σ_α such that $\rho_\alpha(\gamma) = \rho_\alpha(\gamma') = \alpha_i$, and two possibilities arise: either γ and γ' are boundary curves of the same connected component N of Σ_α (like α_1 in Figure 3), or γ is a boundary component of N and γ' is a boundary component of a different connected component N' (like α_2 in Figure 3). In the first case we call α_i a *non-separating limit curve* of N , while in the second case we call it a *separating limit curve* of N and N' .

We denote by $\mathcal{M}_{g,n}$ the mapping class group of Σ , i.e. the group of the isotopy classes of orientation preserving homeomorphisms $h : \Sigma \rightarrow \Sigma$ which fix pointwise the boundary of Σ . Clearly, we have an induced action of $\mathcal{M}_{g,n}$ on the set of the pant decompositions of Σ . We call $\mathcal{M}_{g,n}$ -equivalent two pant decompositions that can be obtained from one another by such action.

Definition 2. A *combinatorial structure* of pant decompositions of $\Sigma_{g,n}$ is a class of $\mathcal{M}_{g,n}$ -equivalence of pant decompositions on $\Sigma_{g,n}$.

Now we can state the following proposition, whose proof is trivial.

Proposition 3. Let $[\alpha] = [\alpha_1, \dots, \alpha_{3g-3+n}]$ and $[\beta] = [\beta_1, \dots, \beta_{3g-3+n}]$ be two isotopy classes of curves defining pant decompositions of Σ . Then the two pant decompositions belong to the same combinatorial structure if and only if there exists a one-to-one correspondence between the components of Σ_α and those of Σ_β and there exists a permutation $\sigma \in S_{3g-3+n}$ such that, for every pair (N, N') where N is any component of Σ_α and N' the corresponding component of Σ_β , we have:

- 1) if γ is an exterior boundary curve of N there exist an exterior boundary curve γ' of N' such that $\rho_\alpha(\gamma) = \rho_\beta(\gamma')$ (i.e. N and N' have the same boundary components);
- 2) if α_i is a separating (resp. non-separating) limit curve of N , then $\beta_{\sigma(i)}$ is a separating (resp. non-separating) limit curve of N' .

In the light of the previous proposition, once a numbering of the boundary components of $\Sigma_{g,n}$ is fixed, any combinatorial structure of pant decompositions of $\Sigma_{g,n}$ can be encoded by its dual graph. This graph has $2g - 2 + n$ trivalent vertices corresponding to pants, and n univalent vertices corresponding to the boundary components. Moreover, the univalent vertices are labelled by $\{1, 2, \dots, n\}$ according to the fixed numbering of the boundary components of $\Sigma_{g,n}$.

The next proposition will be used as a criterion for the simply connectedness of the complexes we are going to construct.

Proposition 4. Let $\pi : C \rightarrow D$ be a surjective cellular map between 2-dimensional CW complexes. Suppose the following conditions are satisfied:

- 1) for any vertex $v \in D$, the fiber $\pi^{-1}(v)$ is connected and simply connected in C ;
- 2) for any oriented edge $e : v_1 \rightarrow v_2$ in D and any two liftings $e' : v'_1 \rightarrow v'_2$ and $e'' : v''_1 \rightarrow v''_2$ of e in C , there exist two paths $\gamma_1 : v'_1 \rightarrow v''_1$ in the fiber $\pi^{-1}(v_1)$ and $\gamma_2 : v'_2 \rightarrow v''_2$ in the fiber $\pi^{-1}(v_2)$, such that the square

$$\begin{array}{ccc} v'_1 & \xrightarrow{e'} & v'_2 \\ \gamma_1 \downarrow & & \downarrow \gamma_2 \\ v''_1 & \xrightarrow{e''} & v''_2 \end{array}$$

is contractible in C .

Then, if D is simply connected, C is simply connected as well.

The proof of this proposition is straightforward, and it is left to the reader.

3. THE COMBINATORIAL STRUCTURES OF PANT DECOMPOSITIONS

This section is devoted to the construction of a simply connected complex $\mathcal{S}_{g,n}$ whose vertices represent the combinatorial structures of pant decompositions of $\Sigma_{g,n}$ or equivalently their dual graphs, as we said in the previous section. Moreover, in the last subsection we will lift the complex $\mathcal{S}_{g,n}$ to another one, denoted by $\tilde{\mathcal{S}}_{g,n}$, codifying all of *decorated combinatorial structures*, i.e. the combinatorial structures

of pant decompositions whose curves are ordered. This is a technical tool which will be needed in Section 4.

We define $V(\mathcal{S}_{g,n})$ to be the set of all connected graphs with n univalent vertices, also called *free ends*, and $2g-2+n$ trivalent vertices. A standard computation shows that each of these graphs has $3g-3+2n$ edges, n connecting a free end to a trivalent vertex, and the remaining $3g-3+n$ connecting two (possibly coinciding) trivalent vertices.

On such graphs we consider the local move shown in Figure 4, that we call *combinatorial F move*, according to the literature, as it can be thought as the fusion of two adjacent trivalent vertices followed by the inverse of a similar fusion. We warn the reader that the graphs in this picture, as well as in the following ones, should be considered as abstract graphs, regardless of their planar representation.

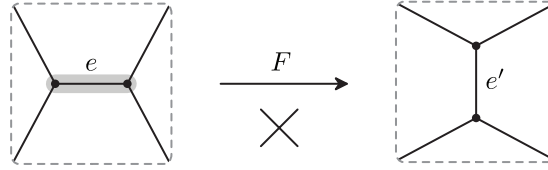


FIGURE 4. The combinatorial F move.

The picture means that the graph is unchanged outside a regular neighborhood of an edge e between two distinct trivalent vertices, while such edge is replaced with a new edge e' , connecting two new trivalent vertices. To be more precise, let v_1 and v_2 be the trivalent vertices connected by the edge e on which we perform the F move. Then, for each i , there are two (possibly coinciding) edges other than e having v_i as a vertex. We label those connected to v_1 by a and b , and those connected to v_2 by c and d . Thus, the starting graph represents the coupling $(ab)(cd)$. Therefore, for each edge between trivalent vertices there are exactly two possible ways to perform the F move (i.e. two possible results for the F move), corresponding to the two possible changes of coupling:

$$\begin{aligned} (ab)(cd) &\rightarrow (ad)(bc); \\ (ab)(cd) &\rightarrow (ac)(bd). \end{aligned}$$

The F move is oriented and in the pictures we mark the starting edge e on which the move is performed by surrounding it by a grey region.

To emphasize that the F move can be realized as the contraction of the edge e followed by the inverse of a similar contraction of the edge e' , we will label the arrows representing F moves by the corresponding intermediate graphs.

Now, we define $\mathcal{S}_{g,n}$ to be the complex having $V(\mathcal{S}_{g,n})$ as the set of vertices, an undirected edge connecting any two vertices which are related by a combinatorial F move, and the following 2-cells:

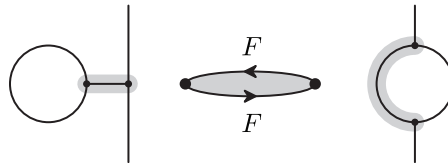


FIGURE 5. A bigon.

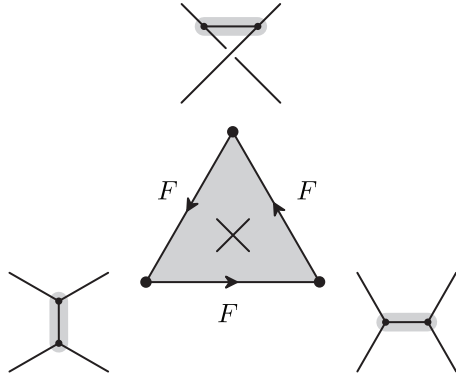


FIGURE 6. A triangle.

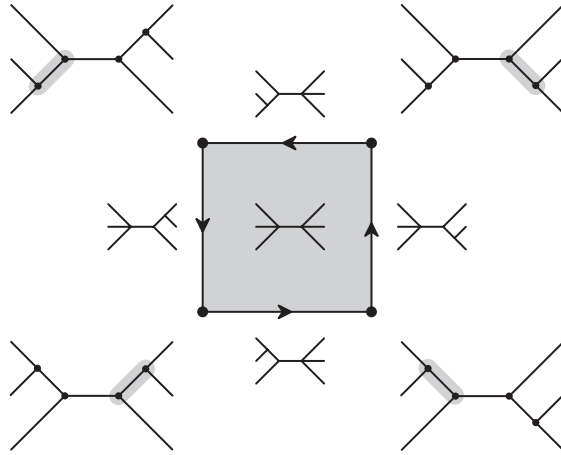


FIGURE 7. A DC square.

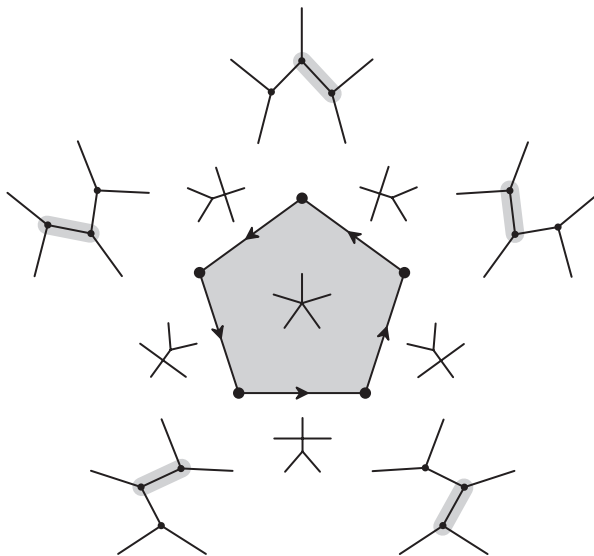


FIGURE 8. A pentagon.

bigons, as in Figure 5;
triangles, as in Figure 6;
squares of “disjoint commutativity” (DC squares), as in Figure 7;
pentagons, as in Figure 8.

Coherently with what we have done for the edges, we consider only one two cell for each loop of edges as in the Figures, even if the same loop may be represented by different sequences of F moves.

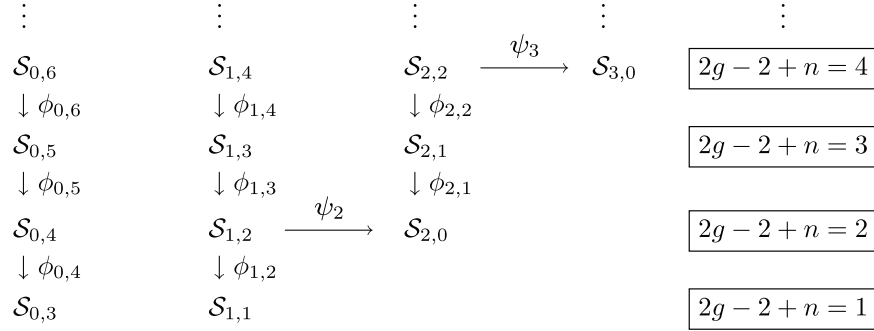
Remark 5. Notice that triangles appear for $2g - 2 + n \geq 2$, squares and pentagons show up when $2g - 2 + n \geq 3$, while bigons are required for $g \geq 1$.

Remark 6. The arrows appearing in the pictures do not represent an orientation for the edges, but they are only intended to specify the oriented F move we are considering.

The main result of this section is the following.

Theorem 7. *The complex $\mathcal{S}_{g,n}$, with $2g - 2 + n \geq 1$, is simply connected.*

The proof takes the next two subsections and proceeds by an induction scheme based on the diagram below, where the complexes $\mathcal{S}_{g,n}$ are staked in layers corresponding to the value of $2g - 2 + n$.



The base for the inductive argument is provided by the two complexes $\mathcal{S}_{0,3}$ and $\mathcal{S}_{1,1}$, which both consist of a single vertex and are therefore trivially connected and simply connected.

In Subsection 3.1 we define the maps $\phi_{g,n} : \mathcal{S}_{g,n} \rightarrow \mathcal{S}_{g,n-1}$ and show that they satisfy the hypotheses of Proposition 4, in order to derive the simply connectedness of $\mathcal{S}_{g,n}$ from that of $\mathcal{S}_{g,n-1}$ (Proposition 8). On the other hand, the maps $\psi_g : \mathcal{S}_{g-1,2} \rightarrow \mathcal{S}_{g,0}$ are defined in Subsection 3.2 and are used to prove that the simply connectedness of $\mathcal{S}_{g-1,2}$ implies that of $\mathcal{S}_{g,0}$ (Proposition 9).

3.1. Reducing the number of boundary components.

We start by defining the map

$$\phi_{g,n} : \mathcal{S}_{g,n} \rightarrow \mathcal{S}_{g,n-1}.$$

If Γ is a vertex of $\mathcal{S}_{g,n}$, $\phi_{g,n}(\Gamma)$ is the graph obtained from Γ by contracting the last free end as in Figure 9: the result is a connected graph with $n - 1$ free ends in the set $\{1, \dots, n - 1\}$ and $2g - 2 + n - 1$ trivalent vertices, i.e. a vertex of $\mathcal{S}_{g,n-1}$.

As far as the edges are concerned, with the notations introduced at the beginning of this section, we have two possibilities: either $n \notin \{a, b, c, d\}$ or $n \in \{a, b, c, d\}$. In the first case, $\phi_{g,n}(F)$ is defined as the F move between $\phi_{g,n}(\Gamma_1)$ and $\phi_{g,n}(\Gamma_2)$. In the second case, being $\phi_{g,n}(\Gamma_1) = \phi_{g,n}(\Gamma_2)$, we can define $\phi_{g,n}(F) = \phi_{g,n}(\Gamma_i)$, as depicted in Figure 10.

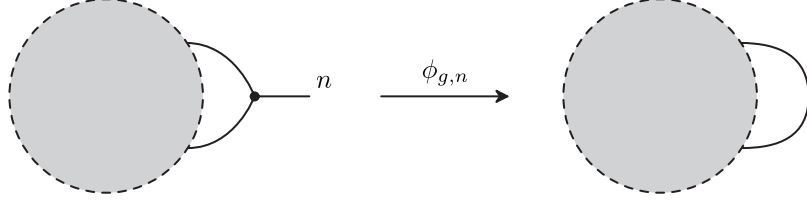


FIGURE 9. Definition of $\phi_{g,n}$ on $V(\mathcal{S}_{g,n})$.

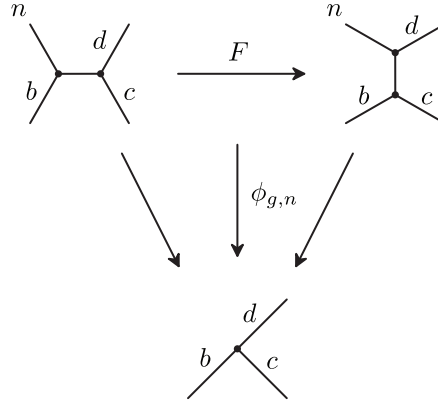


FIGURE 10. Defining $\phi_{g,n}$ on the edges of $\mathcal{S}_{g,n}$.

Finally we define $\phi_{g,n}$ on the 2-cells in the following way. If $\phi_{g,n}$ sends the boundary of a 2-cell of $\mathcal{S}_{g,n}$ onto the boundary of a 2-cell of $\mathcal{S}_{g,n-1}$ having the same shape, then $\phi_{g,n}$ sends the 2-cell of $\mathcal{S}_{g,n}$ in the corresponding one of $\mathcal{S}_{g,n-1}$. Otherwise, it may happen that an edge of the 2-cell collapses to a vertex of $\mathcal{S}_{g,n-1}$, as in Figure 10. If this happens for a bigon or a triangle, then $\phi_{g,n}$ sends the entire boundary to the same vertex, and we send the 2-cell itself to such vertex. On the other hand, if it happens for a square or a pentagon, then the image of the boundary reduces to an edge, and we send all the 2-cell to such an edge.

The map $\phi_{g,n}$ defined in this way is obviously cellular and surjective both on vertices and on edges. To see that it is also surjective on 2-cells, we observe that each 2-cell of $\mathcal{S}_{g,n-1}$ is the image of a 2-cell of $\mathcal{S}_{g,n}$ of the same shape. In fact, the F moves on the boundary of a 2-cell of $\mathcal{S}_{g,n-1}$ always leave a free edge on which the new trivalent vertex can be created, to get the boundary of a 2-cell of $\mathcal{S}_{g,n}$ such that no edge collapses.

Now, we use $\phi_{g,n}$ to get the following inductive step for the proof of Theorem 7.

Proposition 8. *If the complex $\mathcal{S}_{g,n-1}$ is simply connected, then also $\mathcal{S}_{g,n}$ is simply connected, for every g and n such that $2g - 2 + n \geq 2$.*

Proof. The thesis follows by applying Proposition 4 to the map $\phi_{g,n}$, once we prove that the required conditions concerning the preimages of vertices and edges are fulfilled.

Claim 1. *The fiber over each vertex is connected and simply connected in $\mathcal{S}_{g,n}$.*

Let Γ be a vertex of $\mathcal{S}_{g,n-1}$. Then the vertices of $\phi_{g,n}^{-1}(\Gamma)$ consists of all the graphs with n free ends obtained from Γ by inserting an edge with one free end labelled by n and the other end creating a new trivalent vertex along any of the $3g - 3 + 2(n - 1)$ edges of Γ , which is therefore split into two edges (see Figure 11).

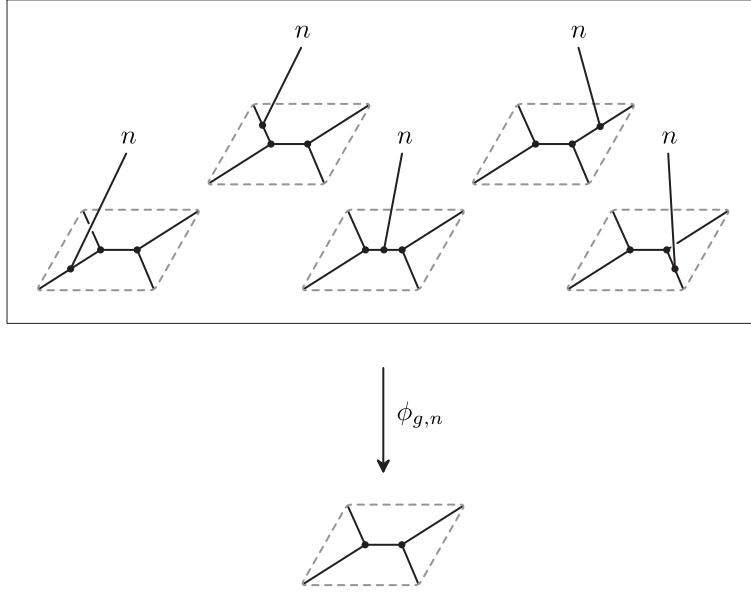


FIGURE 11. The fiber over a vertex.

Notice that two vertices of $\phi_{g,n}^{-1}(\Gamma)$ span an edge in $\phi_{g,n}^{-1}(\Gamma)$ if and only if they are graphs obtained from Γ by inserting the new edge on adjacent edges of Γ , i.e. if and only if they can be obtained from one another by sliding the new trivalent vertex, from one edge of Γ to the adjacent one, through their common trivalent vertex. As explained in Figure 12, this sliding is in fact an F move performed on the marked edge. Then the connectedness of $\phi_{g,n}^{-1}(\Gamma)$ immediately follows from that of Γ .

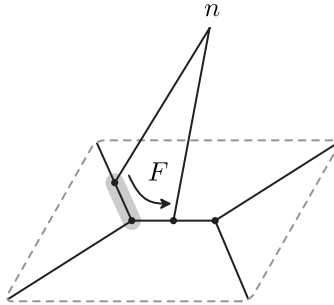


FIGURE 12. The sliding of a trivalent vertex from one edge to the adjacent one is an F move.

The above observation allows us to define a canonical projection from the 1-skeleton of $\phi_{g,n}^{-1}(\Gamma)$ to the graph Γ , once they are barycentrically subdivided. Namely, we project any vertex $\tilde{\Gamma}$ of $\phi_{g,n}^{-1}(\Gamma)$ to the barycenter of the edge of Γ split to get $\tilde{\Gamma}$ as a graph, and the barycenter of any edge $F : \tilde{\Gamma}_1 \rightarrow \tilde{\Gamma}_2$ of $\phi_{g,n}^{-1}(\Gamma)$ to the vertex of Γ shared by the two edges of Γ split to obtain respectively $\tilde{\Gamma}_1$ and $\tilde{\Gamma}_2$. Then, we extend the projection to a cellular map between the two barycentric subdivisions in the obvious way.

Such projection induces a natural one-to-one correspondence between all the paths in $\phi_{g,n}^{-1}(\Gamma)$ and those paths in the barycentric subdivision of Γ whose both ends

are barycenters of edges of Γ . Moreover, this correspondence respects composition and sends loops to loops.

We need to show that any loop γ in any fiber $\phi_{g,n}^{-1}(\Gamma)$, with Γ a vertex of $\mathcal{S}_{g,n-1}$, can be contracted in $\mathcal{S}_{g,n}$ (by getting out of the fiber if needed). The proof is by induction on the length r of γ .

The base of the induction is the case $r = 1$. In this case the loop γ corresponds to an F move which, applied to a graph, produces a new graph equivalent to the original one. This happens when the n -th vertex is attached onto two adjacent edges e_1 and e_2 of Γ , possibly coinciding, which are equivalent by an automorphism of Γ . Figure 13 shows how it is possible to contract such a loop, exploiting the fact that it is one of the three edges of a triangle, whose other two edges coincide.

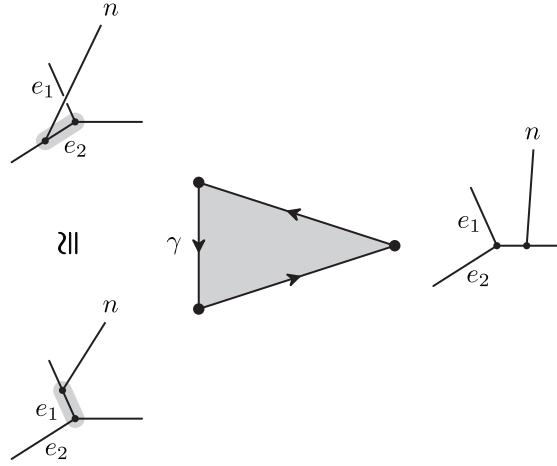


FIGURE 13. A loop γ of length 1 in $\phi_{g,n}^{-1}(\Gamma)$ is contractible in $\mathcal{S}_{g,n}$.

For $r > 1$, the inductive step consists in proving that loop γ is contractible in $\mathcal{S}_{g,n}$, assuming that the same holds for all the loops of length $r - 1$ in any fiber $\phi_{g,n}^{-1}(\Gamma)$.

By means of the one-to-one correspondence introduced above, we can interpret γ as a loop of edges $\hat{\gamma}$ in Γ .

The loop $\hat{\gamma}$ may retrace one of its edges, i.e. may contain an edge of the barycentric subdivision of Γ followed by the same edge with the opposite orientation. This may happen in one of the two cases depicted in Figure 14. In the first situation, the retrace appears in γ as well, and may be canceled. The second situation represents

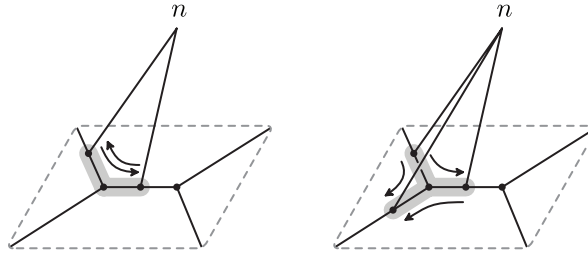


FIGURE 14. Sequences of slidings inducing “retraces” in the loop $\hat{\gamma}$.

a triangle in $\phi_{g,n}^{-1}(\Gamma)$. By homotoping over the corresponding 2-cell, the retrace may be canceled.

After canceling all the retraces, we can assume that the length of γ and $\hat{\gamma}$ coincide.

Now, let us suppose that $\hat{\gamma}$ is not injective: this means that an edge of Γ appears two times in the loop $\hat{\gamma}$. If this is the case, then the loop $\hat{\gamma}$ can be decomposed into two loops of smaller length, inducing a similar decomposition on γ . By induction on the length we are done.

Finally, we are reduced to the case when $\hat{\gamma}$ is an injective loop, i.e. it is a circuit in Γ (see Figure 15).

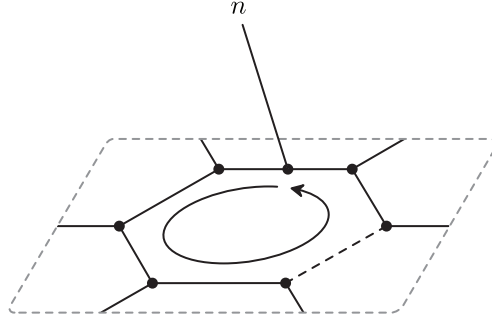


FIGURE 15. A circuit of length r in Γ .

We choose a vertex $\tilde{\Gamma}$ of γ . $\tilde{\Gamma}$ is a vertex of $\mathcal{S}_{g,n}$, obtained from Γ inserting a new edge with a free end in the point n and the other end creating a new trivalent vertex on the edge $e \in \hat{\gamma}$. All the remaining vertices of γ are obtained from Γ inserting the new edge on the $r - 1$ edges of $\hat{\gamma} - \{e\}$. Let us denote by $\tilde{\Gamma}_1$ the vertex which precedes $\tilde{\Gamma}$ and by $\tilde{\Gamma}_2$ the one following it (with respect to the orientation of γ). Those vertices are obtained from Γ by attaching the new edge on the two edges of $\hat{\gamma}$ adjacent to edge e (see Figure 16).

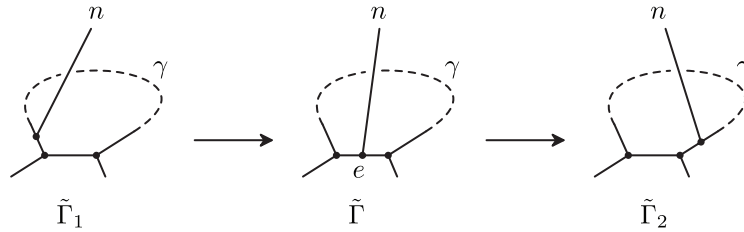


FIGURE 16. Three consecutive vertices of a path $\gamma \in \phi_{g,n}^{-1}(\Gamma)$.

At this point, we apply to all vertices in $\gamma - \{\Gamma\}$ the F move performed on the edge e (F_e in the following), getting from each of them a graph belonging to $\phi_{g,n}^{-1}(F_e(\Gamma))$. The graph $F_e(\Gamma)$ has a circuit of length $r - 1$, and the vertices obtained above are those of the corresponding loop of $\phi_{g,n}^{-1}(F_e(\Gamma))$ (γ_e in Figure 17).

The F move which connects any pair of adjacent vertices in $\gamma - \{\Gamma\}$, together with the two moves F_e departing from such vertices and with the F move connecting their images in $\phi_{g,n}^{-1}(F_e(\Gamma))$, bounds a DC square (see Figure 17).

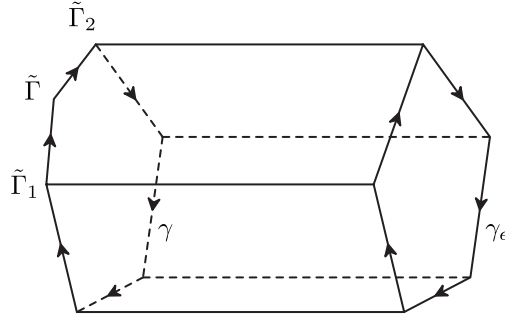


FIGURE 17. Homotoping a loop of length r to a loop of length $r - 1$.

Let us consider the pentagonal loop with vertices $\tilde{\Gamma}_1, \tilde{\Gamma}, \tilde{\Gamma}_2$ (all belonging to $\phi_{g,n}^{-1}(\Gamma)$), $F_e(\tilde{\Gamma}_1)$ and $F_e(\tilde{\Gamma}_2)$ (in $\phi_{g,n}^{-1}(F_e(\Gamma))$). As illustrated in Figure 18, such loop can be filled in with triangles and pentagons.

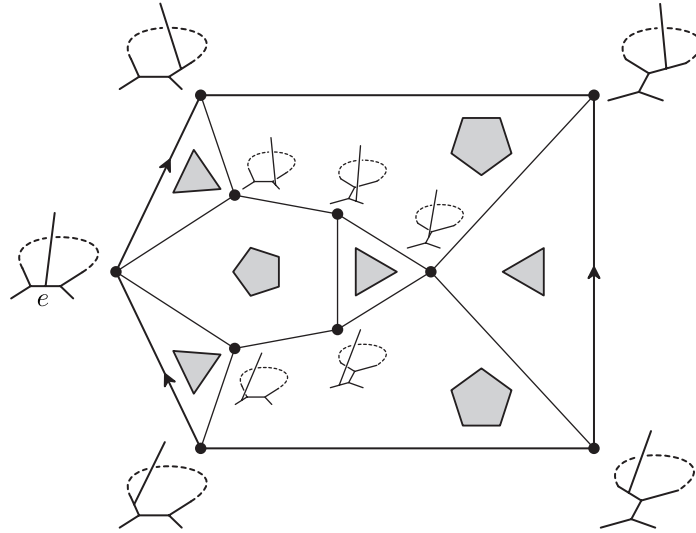


FIGURE 18. The pentagonal loop may be filled in by triangles and pentagons.

The r -sided loop can therefore be homotoped to the $(r - 1)$ -sided one, which is in turn contractible by the inductive hypothesis, from which the thesis follows.

Claim 2. *The condition on the lifting of edges is satisfied.*

Let $E : \Gamma \rightarrow \Gamma'$ be an edge of $\mathcal{S}_{g,n-1}$. Such E is an F move performed on an edge e (with distinct endpoints) of Γ : hence, E has $3g + 2n - 6$ liftings to $\mathcal{S}_{g,n}$, as many as the number of edges in $\Gamma - \{e\}$. Let $E_1 : \Gamma_1 \rightarrow \Gamma'_1$ and $E_2 : \Gamma_2 \rightarrow \Gamma'_2$ be two of these liftings. As $\phi_{g,n}^{-1}(\Gamma)$ is connected, there is a simple path γ in $\phi_{g,n}^{-1}(\Gamma)$ connecting Γ_1 to Γ_2 . The graph Γ_1 is obtained from Γ by inserting a new trivalent vertex on an edge f which is different from e , and connecting it with the new free end n . The path γ consists of consecutive F moves in the fiber, i.e. consecutive slidings of the new trivalent vertex. We concentrate on the first edge of γ , the one departing from Γ_1 . Such edge represents a sliding of the new vertex from edge f to edge g , through the vertex they have in common (i.e. it is an F move in the fiber $\phi_{g,n}^{-1}(\Gamma)$): denoted by Γ_3 the resulting graph, still belonging to $\phi_{g,n}^{-1}(\Gamma)$, three possibilities are given:

- (i) f and e are disjoint;
- (ii) f and e intersect at a vertex, and $g \neq e$;
- (iii) f and e intersect at a vertex, and $g = e$.

In the first case, E admits a lifting $E_3 : \Gamma_3 \rightarrow \Gamma'_3$, and Γ'_3 is obtained from Γ'_1 with the same sliding used to get Γ_3 from Γ_1 . The two liftings of E and the two slidings bound a DC square, and the resulting loop is therefore contractible.

In the second case, E still admits a lifting $E_3 : \Gamma_3 \rightarrow \Gamma'_3$, but to get Γ'_3 from Γ'_1 we need to perform two slidings along consecutive vertices. Then, the two liftings of E and the three slidings bound a pentagon, and the resulting loop is once again contractible (see Figure 19).

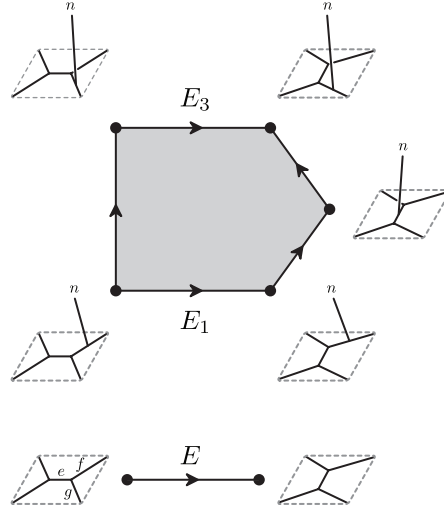


FIGURE 19. Lifting of an edge, Case (ii).

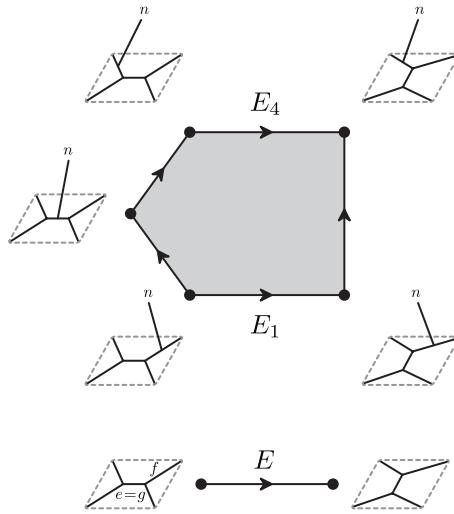


FIGURE 20. Lifting of an edge, Case (iii-a).

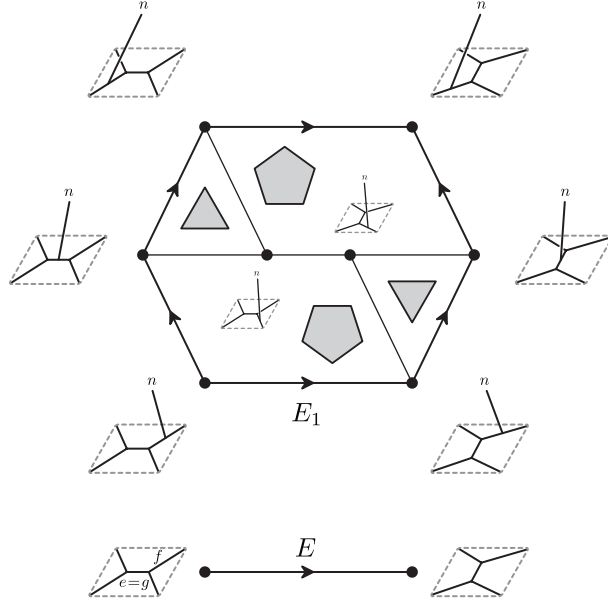


FIGURE 21. Lifting of an edge, Case (iii-b).

In the third case, instead, Γ_3 does not support the F move that lifts E . However, if we slide further, by walking through the following edge in the path γ , we end up with a graph Γ_4 that supports the move. Denoted by $E_4 : \Gamma_4 \rightarrow \Gamma'_4$ the lifting of E starting in Γ_4 , two possibilities are given: either the graph Γ'_4 turns out to be related to Γ'_1 by a single sliding, or two slidings are needed to get Γ'_1 from Γ'_4 . In the former case, the two liftings of E and the three slidings still bound a pentagon, resulting in a contractible loop (see Figure 20). In the latter case, the two liftings and the four slidings give rise to an hexagon. Nevertheless, such an hexagon may be subdivided into triangles and pentagons, as shown in Figure 21, being therefore contractible.

The same argument applies to all consecutive edges of the path γ . We get this way a path γ' in $\phi_{g,n}^{-1}(\Gamma')$ connecting Γ'_2 to Γ'_1 , and the loop bounded by γ , γ' , E_1 and E_2 is contractible by construction. Hence Claim 2 is proved.

This concludes the proof of Proposition 8. \square

3.2. Dealing with the closed case.

A further step needed to prove Theorem 7, is the definition of a map

$$\psi_g : \mathcal{S}_{g-1,2} \rightarrow \mathcal{S}_{g,0} .$$

We define this map as follows. If Γ is a vertex of $\mathcal{S}_{g-1,2}$, then $\psi_g(\Gamma)$ is the graph obtained from Γ by attaching its two free ends together, as shown in Figure 22. Such a graph turns out to have $2g - 2$ trivalent vertices and no free ends, i.e. it is a vertex of $\mathcal{S}_{g,0}$. Now, every edge of $\mathcal{S}_{g-1,2}$ is an F move connecting two graphs $\Gamma_1, \Gamma_2 \in V(\mathcal{S}_{g-1,2})$. Then there exists an F move between $\psi_g(\Gamma_1)$ and $\psi_g(\Gamma_2)$, and we define $\psi_g(F)$ to be such a move. The definition of ψ_g on the 2-cells is straightforward.

The map ψ_g we have just defined is cellular. It allows us to obtain the second inductive step for the proof of Theorem 7.

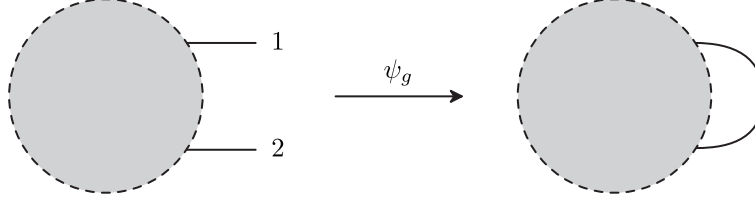


FIGURE 22. Definition of ψ_g on $V(\mathcal{S}_{g-1,2})$.

Proposition 9. *If the complex $\mathcal{S}_{g-1,2}$ is simply connected, then also $\mathcal{S}_{g,0}$ is simply connected, for every $g > 1$.*

Proof. We observe that ψ_g can be easily seen to be surjective, by the same argument used for the surjectivity of $\phi_{g,n}$, except that here the free edge is the one to be cut to get liftings of cells. Then the connectedness of $\mathcal{S}_{g-1,2}$ implies that of $\mathcal{S}_{g,0}$, and the proposition immediately follows from the following claim.

Claim 1. *For any loop of edges γ in $\mathcal{S}_{g,0}$ there exists a loop of edges $\tilde{\gamma}$ in $\mathcal{S}_{g-1,2}$, such that $\psi_g \circ \tilde{\gamma}$ is homotopic to γ in $\mathcal{S}_{g,0}$.*

In order to prove this claim, we need another claim.

Claim 2. *For any vertex Γ of $\mathcal{S}_{g,0}$ and any two vertices Γ_1 and Γ_2 in $\psi_g^{-1}(\Gamma)$, there exists a path of edges δ in $\mathcal{S}_{g-1,2}$ between Γ_1 and Γ_2 , such that the loop $\lambda = \psi_g \circ \delta$ is homotopically trivial in $\mathcal{S}_{g,0}$.*

We first prove Claim 1 assuming Claim 2. We choose a vertex Γ of $\mathcal{S}_{g,0}$ as the base point for the loop γ , and denote by Γ_0 the vertex of $\psi_g^{-1}(\Gamma)$, which is obtained from Γ by cutting it along an edge e_0 .

We choose Γ_0 as the basepoint of the lifting $\tilde{\gamma}$ and consider the first edge of γ , i.e. the one departing from Γ . Such edge is an F move performed on an edge e of Γ . If $e \neq e_0$, then we can lift the move F_e to a move on Γ_0 . On the contrary, if $e = e_0$ then the move F_e cannot be lifted to a move on the graph Γ_0 and we apply Claim

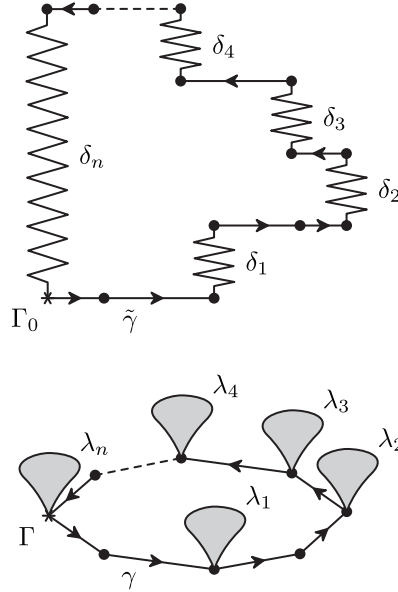


FIGURE 23. The path $\tilde{\gamma}$ and its projection in $\mathcal{S}_{g,0}$.

2 in order to connect Γ_0 with a different vertex of $\psi_g^{-1}(\Gamma)$ on which the move F_e can be lifted.

We go on to construct our lifting, by following γ edge after edge and iterating the procedure described for the first edge.

In this way we end up with a path joining Γ_0 with some other vertex of $\psi_g^{-1}(\Gamma)$ and we can close it to get the desired loop $\tilde{\gamma}$ by applying once again Claim 2. The scenario is that of Figure 23.

Then $\psi_g \circ \tilde{\gamma}$ differs from γ only for the insertion of some homotopically trivial loops $\lambda_i = \psi_g \circ \delta_i$, one for each application of Claim 2. Therefore, $\psi_g \circ \tilde{\gamma}$ is homotopic to γ as required by Claim 1.

Now we pass to prove Claim 2. Let Γ_1 and Γ_2 be obtained from Γ respectively by cutting two different edges e_1 and e_2 .

If e_1 and e_2 share both the ends, then $\Gamma_1 = \Gamma_2$ (see rightmost graphs in Figure 24) and there is nothing to prove.

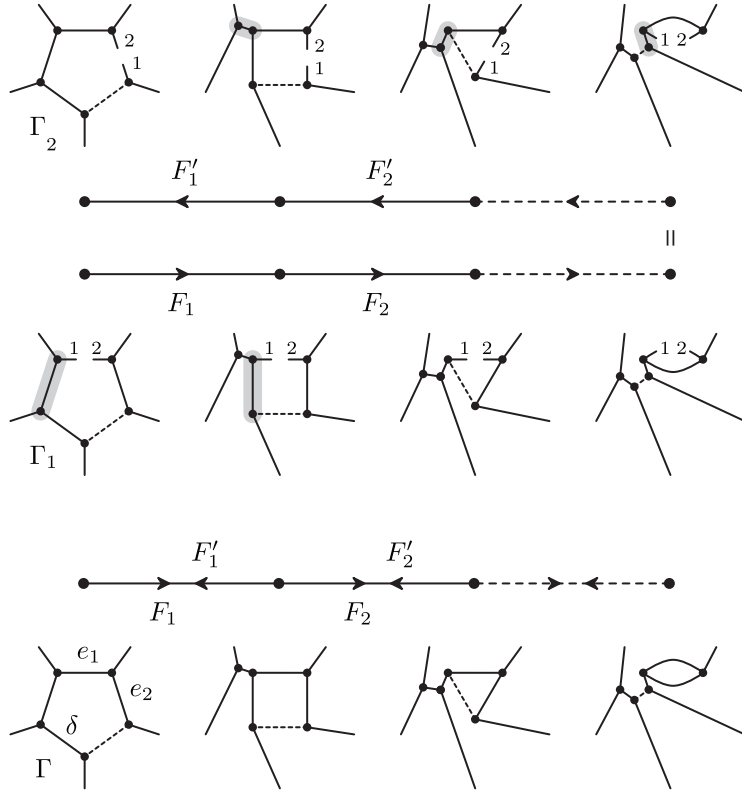


FIGURE 24. The path $\psi_g \circ \tilde{\delta}$ is contractible in $\mathcal{S}_{g,0}$.

Otherwise, if e_1 and e_2 do not share both ends but are still adjacent, then the fact that both can be cut without disconnecting Γ ensures the existence of a simple path of edges δ in $\Gamma - \{e_1, e_2\}$ joining two different vertices of e_1 and e_2 , as in Figure 24. The same figure suggests how to construct the desired path δ as a sequence of liftings of F moves performed in the order on the edges of δ , followed by a sequence of liftings of their inverses in the reversed order. Then the loop $\lambda = \psi_g \circ \delta$ turn out to be homotopically trivial by construction.

Finally, if e_1 and e_2 are not adjacent, then we consider a minimal path of edges ϵ in Γ between a (trivalent) vertex v_1 of e_1 and a vertex v_2 of e_2 . By performing F

moves on the edges of ϵ in the order, we can drag v_1 until it coincides with v_2 . In this way we get a path of edges $\hat{\epsilon}$ in $\mathcal{S}_{g,0}$ connecting Γ with a new graph Γ' where e_1 and e_2 are adjacent. Since neither e_1 nor e_2 can appear in ϵ , we can lift $\hat{\epsilon}$ to paths $\hat{\epsilon}_1$ and $\hat{\epsilon}_2$ in $\mathcal{S}_{g-1,2}$ respectively starting from Γ_1 and Γ_2 . Now, calling Γ'_1 and Γ'_2 the end points of these two paths in $\psi_g^{-1}(\Gamma')$, we are reduced to the previous case. Therefore, we can find a path of edges δ' between Γ'_1 and Γ'_2 such that the loop $\lambda' = \psi_g \circ \delta'$ is contractible in $\mathcal{S}_{g,0}$. Then we put $\delta = \hat{\epsilon}_1 \delta' \hat{\epsilon}_2^{-1}$ and observe that once again the loop $\lambda = \psi_g \circ \delta = \epsilon \lambda' \epsilon^{-1}$ is homotopically trivial by construction. \square

3.3. The decorated combinatorial structures.

As anticipated, we conclude this section with the construction of the complex $\tilde{\mathcal{S}}_{g,n}$, codifying all of *decorated combinatorial structures*, i.e. the combinatorial structures of pant decompositions whose curves are ordered.

Let $V(\tilde{\mathcal{S}}_{g,n})$ be the set of all connected graphs with n univalent vertices and $2g - 2 + n$ trivalent vertices, equipped with an ordering of the $3g - 3 + n$ edges connecting two trivalent vertices. For those graphs we may define a *decorated F move*, naturally lifting the combinatorial F move defined in Section 3, simply requiring that the new edge created by the F move inherits its number by the old one. In order to emphasize that the F move is performed on the i -th edge, we denote it by F_i . Moreover, if two decorated graphs are identical except for the ordering of the edges, which differ by a transposition $(ij) \in \Sigma_{3g-3+n}$, we connect them with an edge, labeled by τ_{ij} . We complete the construction by adding 2-cells of three types: *combinatorial*, *algebraic* and *mixed* ones.

The combinatorial 2-cells translate in terms of decorated combinatorial structures the bigons, triangles, squares and pentagons of $\mathcal{S}_{g,n}$. Notice that the shape of the bigons and that of the pentagons change when lifted to the decorated setting, as depicted in Figure 25, while all the other combinatorial cells maintain their shape.

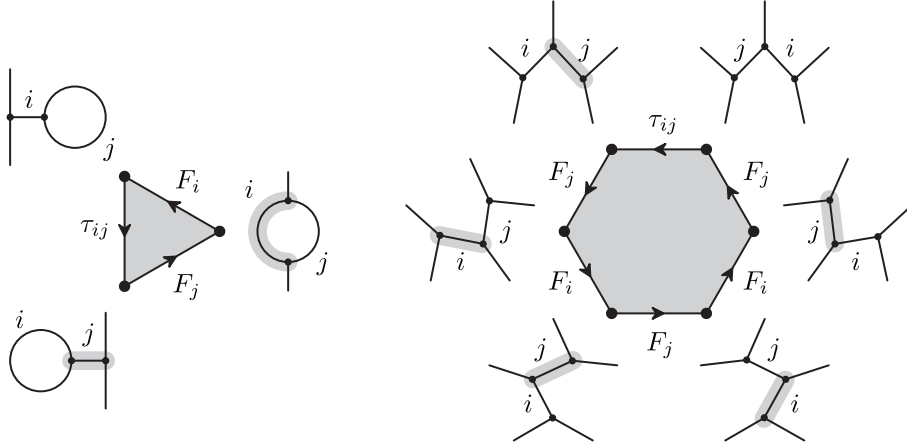


FIGURE 25. A bigon and a pentagon of decorated F moves.

The algebraic 2-cells correspond to the relation in the group Σ_{3g-3+n} , thus they are squares $\tau_{ij}\tau_{hk}\tau_{ij} = \tau_{lm}$, for any couple of different transpositions (ij) and (hk) in Σ_{3g-3+n} , where $(lm) = (ij)(hk)(ij)$.

Finally, the mixed two cells are squares $F\tau_{ij} = \tau_{ij}F$, telling that F and τ moves commute.

The complex $\tilde{\mathcal{S}}_{g,n}$ built like that has an obvious projection on $\mathcal{S}_{g,n}$, which is defined on the vertices by forgetting the ordering and extends to edges and 2-cells

in a natural way. Proving that such map satisfies all the hypothesis of Proposition 4 is straightforward, and we leave it to the reader. The application of Proposition 4 thus ensures that $\tilde{\mathcal{S}}_{g,n}$ is connected and simply connected.

4. THE COMPLEX OF PANT DECOMPOSITIONS

In this section we want to lift the complex $\mathcal{S}_{g,n}$ to a new complex $\mathcal{R}_{g,n}$, whose vertices are in one-to-one correspondence with the *pant decompositions* of the surface $\Sigma_{g,n}$. This result is achieved in two steps, described in the two subsections: first of all, we define a complex $\tilde{\mathcal{R}}_{g,n}$, whose vertices are in one-to-one correspondence with the decorated pant decompositions of $\Sigma_{g,n}$, in such a way that the natural action of the mapping class group $\mathcal{M}_{g,n}$ on the decorated pant decompositions extends to an action on $\tilde{\mathcal{R}}_{g,n}$ and the quotient $\tilde{\mathcal{R}}_{g,n}/\mathcal{M}_{g,n}$ coincides with $\tilde{\mathcal{S}}_{g,n}$. Provided we take care that the natural projection $r_{g,n} : \tilde{\mathcal{R}}_{g,n} \rightarrow \tilde{\mathcal{S}}_{g,n}$ satisfies the conditions of Proposition 4, the new complex turns out to be simply connected. Finally, we exploit the natural projection $t_{g,n} : \tilde{\mathcal{R}}_{g,n} \rightarrow \mathcal{R}_{g,n}$ to prove that $\mathcal{R}_{g,n}$ is simply connected as well.

4.1. The decorated pant decompositions.

As anticipated in the introduction, we need now a presentation for all the mapping class groups. In order to produce such presentation, we use the results of [4]. In such paper a machinery for finding presentations is built; its input is a presentation for the mapping class group of the sphere with 4 and 5 boundary components, and for the torus with 1 and 2 boundary components (*sporadic surfaces*). Moreover, [4] also shows that such a machinery produces a presentation of any known “style”, provided the input is chosen according to the same “style”. In order to perform the explicit calculations shown in this section, it is convenient to use a presentation in terms of Dehn twists, described by Gervais in [7], that we may obtain with the above recalled method starting from the *Dehn twist style* presentations for the sporadic surfaces.

The generators in such a presentation are the Dehn twists along all simple closed curves in $\Sigma_{g,n}$, while the relations belong to three simple types, *braids*, *lanterns* and *chains*.

Namely, we call *braids* the relations of the form

$$T_c = T_b T_a T_b^{-1},$$

where the curves a and b are such that $|a \cap b| = 0, 1$ or $|a \cap b| = 2_0$ (meaning they intersect in two points with algebraic intersection zero), and $c = T_b(a)$.

We call *lanterns* the relations like

$$T_{a_1} T_{a_2} T_{a_3} T_{a_4} = T_{d_{12}} T_{d_{23}} T_{d_{13}},$$

where the curves a_i, d_{ij} are represented in Figure 26.

Finally, we name *chains* the relations

$$(T_{a_1} T_b T_{a_2})^4 = T_{c_1} T_{c_2},$$

where a_i, c_j are the curves depicted in Figure 27.

The vertices of $\tilde{\mathcal{R}}_{g,n}$ have to be in a one to one correspondence with the (infinitely many) decorated pant decompositions of $\Sigma_{g,n}$, i.e.

$$V(\tilde{\mathcal{R}}_{g,n}) = \{\text{decorated pant decompositions of } \Sigma_{g,n}\} / \text{isotopy}$$

We now define a transformation between decorated pant decompositions, that we call again *F move*. Let D be the decorated pant decomposition given by an ordered family $\{a_1, \dots, a_{3g-3+n}\}$ of curves (up to isotopy). Let us consider one of these curves, a_i , and let a'_i be any curve on Σ such that $|a_i \cap a'_i| = 2_0$ and

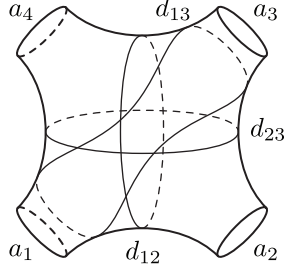


FIGURE 26. Lanterns are supported in subsurfaces homeomorphic to $\Sigma_{0,4}$.

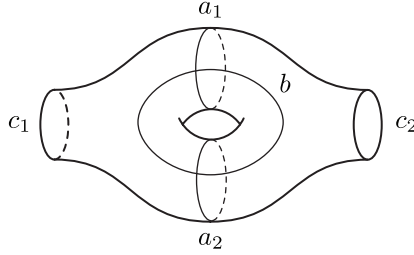


FIGURE 27. Chains are supported in subsurfaces homeomorphic to $\Sigma_{1,2}$.

$D' = \{a_1, \dots, a'_i, \dots, a_{3g-3+n}\}$ is still a decorated pant decomposition. The move F is defined as the transformation

$$D = \{a_1, \dots, a_i, \dots, a_{3g-3+n}\} \xrightarrow{F} D' = \{a_1, \dots, a'_i, \dots, a_{3g-3+n}\}.$$

In order to emphasize that such F move is performed on the i -th curve of D , we denote it by F_i .

The move, depicted in Figure 28, is a transformation between decorated pant decompositions of $\Sigma_{g,n}$, supported in a subsurface homeomorphic to a sphere with four boundary components, i.e. it is a local move.

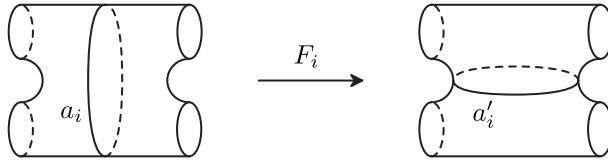


FIGURE 28. The F move between decorated pant decompositions.

We connect two vertices in $V(\tilde{\mathcal{R}}_{g,n})$ by an edge F if the corresponding decompositions are related to one another by an F move. Moreover, we insert an edge τ_{ij} between two vertices if the corresponding decompositions are identical but for the ordering of the curves, which differ by the transposition τ_{ij} , $i, j = 1, \dots, 3g - 3 + n, i \neq j$. Finally, we insert an edge T_a between two vertices if the corresponding decompositions are related to one another by the Dehn twist along a simple closed curve a .

To the 1-dimensional complex obtained above, we now add 2-cells of *combinatorial*, *algebraic*, *topological* and *mixed* type.

The combinatorial 2-cells rephrase in terms of pant decompositions the bigons, triangles, squares and pentagons of $\tilde{\mathcal{S}}_{g,n}$. Once again, the shape of the bigons

changes when lifted from the combinatorial setting to the new one, as depicted in Figure 29, while all the other combinatorial cells maintain their shape.

The algebraic 2-cells correspond to the relations of the symmetric group over $3g - 3 + n$ elements, hence they are squares of τ moves.

The topological 2-cells are the ones carried by the relations in the Dehn twist presentation of $\mathcal{M}_{g,n}$ (braids, lanterns and chains), together with the squares of T moves shown in Figure 30. We also see that a twist, when performed on a curve which does not intersect any of the curves belonging to D , produces a loop of length 1 based in the vertex of $\tilde{\mathcal{R}}_{g,n}$ corresponding to D . If we then fill also these loops with 2-cells, we obtain a third type of topological 2-cells.

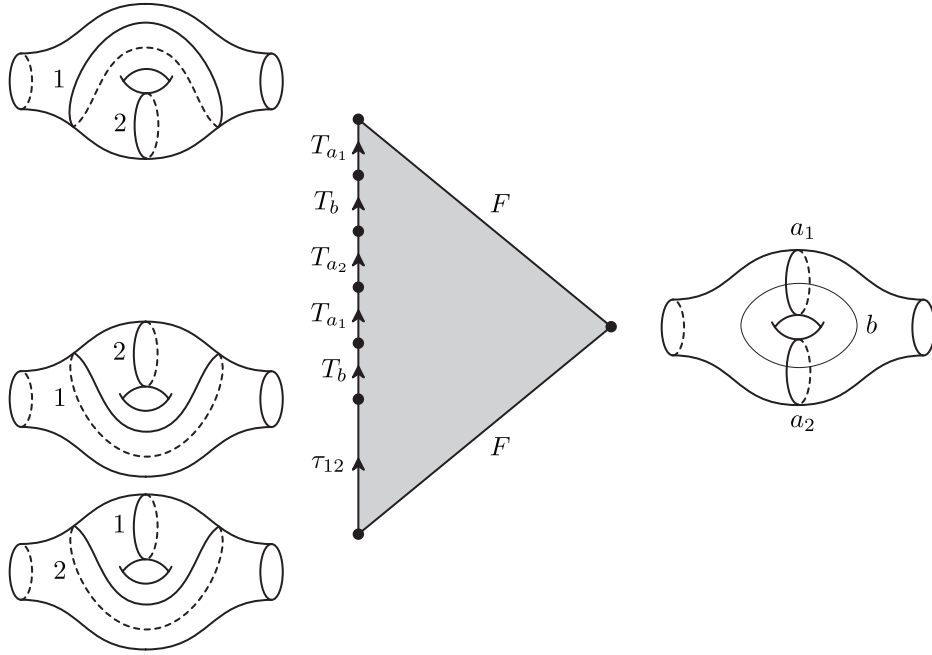


FIGURE 29. A bigon of decorated pant decompositions.

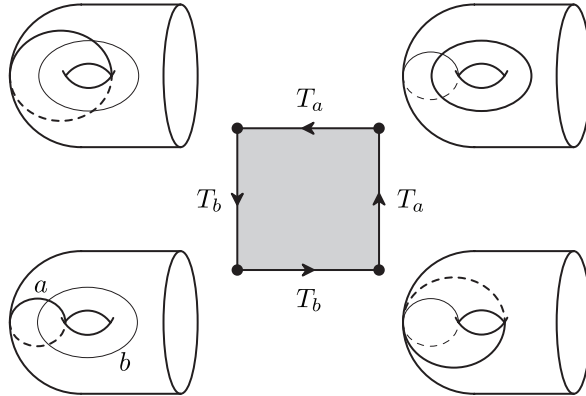


FIGURE 30. A square of T moves.

Finally, the mixed 2-cells are the triangles shown in Figure 31, the squares telling that the F moves commute with the Dehn twists and with the τ moves, and those telling that Dehn twist and τ moves commute as well.

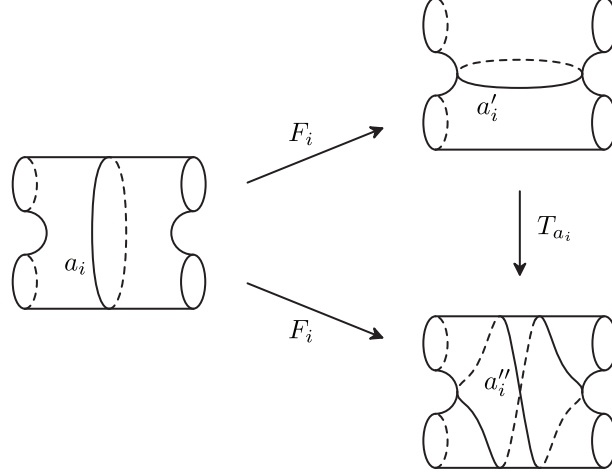


FIGURE 31. Mixed triangles.

We define $\tilde{\mathcal{R}}_{g,n}$ to be the complex having $V(\tilde{\mathcal{R}}_{g,n})$ as the set of vertices, edges and 2-cells as above. We may now state the following result, whose proof takes up the remainder of this subsection.

Theorem 10. *The complex $\tilde{\mathcal{R}}_{g,n}$ is simply connected.*

Proof. To prove the theorem, we consider the map $r_{g,n} : \tilde{\mathcal{R}}_{g,n} \rightarrow \tilde{\mathcal{S}}_{g,n}$ defined as follows. On the vertices, $r_{g,n}$ is the natural projection associating to any decorated pant decomposition the corresponding decorated combinatorial structure. As far as the edges are concerned, $r_{g,n}$ sends each F and each τ_{ij} between two decompositions in the combinatorial F and τ_{ij} between the corresponding combinatorial structures, and contracts each Dehn twist T_a to a point. The map so defined extends to a map $r_{g,n} : \tilde{\mathcal{R}}_{g,n} \rightarrow \tilde{\mathcal{S}}_{g,n}$, which is surjective thanks to the combinatorial and the algebraic 2-cells and to the squares $F\tau = \tau F$ inserted in $\tilde{\mathcal{R}}_{g,n}$.

We are then left to check that the remaining hypotheses of Proposition 4 are fulfilled.

Claim 1. *The fiber over each vertex is connected and simply connected in $\mathcal{T}_{g,n}$.*

Let Γ be a vertex of $\tilde{\mathcal{S}}_{g,n}$, i.e a combinatorial structure of decorated pant decomposition. Then,

$$r_{g,n}^{-1}(\Gamma) = \{\text{decorated pant decompositions with combinatorial structure } \Gamma\}$$

Given one element of $r_{g,n}^{-1}(\Gamma)$, any other is obtained from the selected one via the action of the mapping class group. The set $r_{g,n}^{-1}(\Gamma)$ is therefore connected, since the edges of $\tilde{\mathcal{R}}_{g,n}$ include all the Dehn twists.

We need to prove that $r_{g,n}^{-1}(\Gamma)$ is simply connected. Since every element γ in $\mathcal{M}_{g,n}$ defines a corresponding path in $r_{g,n}^{-1}(\Gamma)$, which is unique up to homotopy in the fiber, such path will be denoted by γ as well. Let γ be a loop in $r_{g,n}^{-1}(\Gamma)$, and let D be its basepoint. There are two possibilities: either γ is a trivial element in $\mathcal{M}_{g,n}$, or it is a nontrivial element of $\text{Stab}(D) \subset \mathcal{M}_{g,n}$. In the former case, γ is contractible due to the topological 2-cells, representing the relations of the mapping class group.

In fact, γ is a relation in $\mathcal{M}_{g,n}$, then it follows from the braids, lanterns and chains. Let then γ represent a nontrivial element of $\text{Stab}(D) \subset \mathcal{M}_{g,n}$. In particular, γ sends each curve of D in itself, possibly inverting its orientation.

If γ respects the orientation of all the curves in D , then it may be expressed (i.e. is equivalent in $\mathcal{M}_{g,n}$) as the product of Dehn twists performed over the curves a_i of the decomposition D . By means of the relations of $\mathcal{M}_{g,n}$, the loop γ may be homotoped in $r_{g,n}^{-1}(\Gamma)$ to the product of the corresponding loops, i.e.

$$\gamma \sim \prod_i T_{a_i}.$$

Such loops are in turn contractible, because we cupped them off by the corresponding 2-cells, thus ensuring that γ is contractible as well.

Let us suppose that γ respects the ordering of the curves in D , but it changes the orientation of one of them, a_i . Thus, a_i cannot be a separating curve of $\Sigma_{g,n}$: in fact, if a_i was separating, then γ should switch the two connected components of $\Sigma_{g,n} - a_i$. Then, γ would switch at least two curves in D , or two components of $\partial\Sigma_{g,n}$, which is impossible.

Hence, a_i is non-separating and two possibilities are given: either a_i bounds on both sides the same pant P , or a_i bounds a pant P on one side and a pant P' on the other.

In the first situation, the homeomorphism γ may be represented by the product $\omega_i \cdot \prod_j T_{a_j}$, where the a_j 's are curves of D and ω_i is the semitwist of P relative to a_i . It is well known that such a semitwist may be expressed by the product $T_b T_{a_i}^2 T_b$, where b is as shown in Figure 30). Hence the loop γ is homotopic in $r_{g,n}^{-1}(\Gamma)$ to the product of the corresponding loops, i.e.

$$\gamma \sim T_b T_{a_i}^2 T_b \prod_j T_{a_j}.$$

The loop corresponding to the semitwist is contractible (indeed it is the boundary of a square of T moves), and so are the others, ensuring this way that γ is contractible as well.

In the second situation, γ switches the two pants bounded by a_i , P and P' . Since γ does not permute the curves of D , also the remaining boundary components of P and P' must be in common. Hence, $\Sigma_{g,n} = \Sigma_{2,0}$, D is as shown in Figure 32 and γ is the rotation of π radians around the horizontal axis.

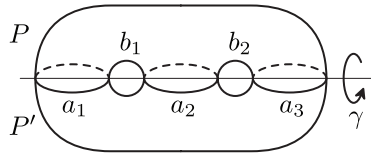


FIGURE 32. The rotation γ .

We remark that all the loops we considered so far are contractible without getting out of their own fiber, which is any one among the $r_{g,n}^{-1}(\Gamma)$. Conversely, in the case of the rotation depicted in Figure 32 it is required to get out of the fiber, as described in the following lemma.

Lemma 11. *Let γ be the homeomorphism of $\Sigma_{2,0}$ switching P and P' (notations as in Figure 32). Then the corresponding loop of $r_{2,0}^{-1}(\Gamma)$ is contractible in $\tilde{\mathcal{R}}_{2,0}$.*

Proof. The homeomorphism γ may be expressed in terms of Dehn twists as the product $\gamma = (T_{b_2}T_{a_3}^2T_{b_2})^{-1}T_{b_1}T_{a_1}^2T_{b_1}$ (up to twists along the curves of D). Let us perform, starting from D , an F move along the curve a_2 , and let us denote by D' the resulting pant decomposition. The homeomorphism γ , applied to D' , gives rise to a contractible loop, as shown in Figure 33.

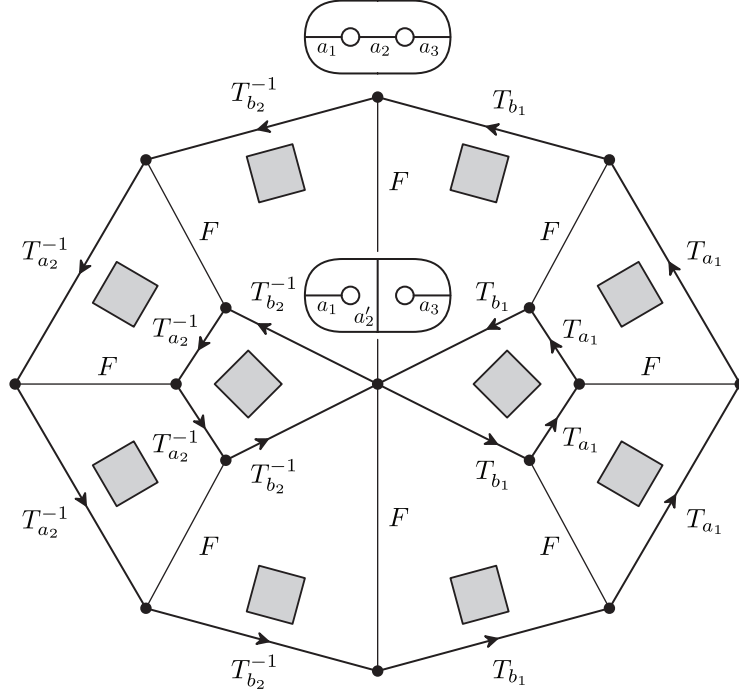


FIGURE 33. Contracting the loop γ in $\tilde{\mathcal{R}}_{2,0}$.

The same picture shows that the original loop γ is homotopic, by means of the mixed squares, to that contractible loop, thus proving the thesis. \square

In conclusion, if γ inverts the orientation of more than one curve of D , then either we are in the situation of the lemma (hence γ is contractible) or all curves whose orientation is changed by γ bound on both sides the same pant. In the latter case, γ may be expressed as the product of Dehn twists performed over the curves a_i and of semitwists ω_j relative to the a_j 's whose orientation is changed. By means of the relations of $\mathcal{M}_{g,n}$, the loop γ may be homotoped in $r_{g,n}^{-1}(\Gamma)$ to the product of the corresponding loops, i.e.

$$\gamma \sim \prod_i T_{a_i} \prod_j \omega_j.$$

Such loops are in turn contractible, since we cupped them off by the corresponding 2-cells, and this concludes the proof of Claim 1.

Claim 2. *The condition on the lifting of edges is satisfied.*

The edges of $\tilde{\mathcal{S}}$ are F and τ moves. Each of these edges has infinitely many liftings to $\tilde{\mathcal{R}}$, and the lifting condition follows almost trivially by the mixed 2-cells.

Namely, let us consider a decorated combinatorial F move, F_i , performed on an edge e_i , that transforms the graph Γ_1 into the graph Γ_2 . Let us consider two

different liftings of the F_i move, $F'_i : D'_1 \rightarrow D'_2$ and $F''_i : D'_1 \rightarrow D'_2$. Given a path δ_1 in $r_{g,n}^{-1}(\Gamma_1)$ connecting D'_1 to D'_1 , the same path connects D'_2 to a D_2 in $r_{g,n}^{-1}(\Gamma_2)$. Such D_2 coincides with D'_2 except, possibly, for the i -th curve. D_2 and D'_2 are then connected by a power of $T_{a'_i}$. The path δ_2 , which is the composition of δ_1 with the suitable power of $T_{a'_i}$, connects D'_2 to D'_2 in $r_{g,n}^{-1}(\Gamma_2)$, and the square bounded by F'_i, F''_i, δ_1 and δ_2 is contractible due to the mixed squares and triangles. If $D'_1 = D'_1$, then D'_2 and D'_2 simply differ by a multiple of $T_{a'_i}$. Thus, the loop $F''_i T_{a'_i}^k (F'_i)^{-1}$ is contractible due to the mixed triangles.

The proof of the analogous condition for the lifting of edges of type τ is straightforward, provided we remark that such moves commute with all Dehn twists and that we inserted all the corresponding DC squares.

All conditions of Proposition 4 are fulfilled. The thesis of Theorem 10 has therefore been demonstrated. \square

4.2. Back to pant decompositions.

The final step of our construction consists in the definition of a complex $\mathcal{R}_{g,n}$, with all the pant decompositions of $\Sigma_{g,n}$ as the set of vertices, such that two maps $t_{g,n} : \tilde{\mathcal{R}}_{g,n} \rightarrow \mathcal{R}_{g,n}$ and $p_{g,n} : \mathcal{R}_{g,n} \rightarrow \mathcal{S}_{g,n}$ are defined and the diagram

$$\begin{array}{ccc} \tilde{\mathcal{R}}_{g,n} & \xrightarrow{t} & \mathcal{R}_{g,n} \\ r \downarrow & & \downarrow p \\ \tilde{\mathcal{S}}_{g,n} & \xrightarrow{s} & \mathcal{S}_{g,n} \end{array}$$

(where s is the natural projection) is commutative. The core result of this last section is the proof that the simply connectedness of $\mathcal{R}_{g,n}$ follows directly from that of $\tilde{\mathcal{R}}_{g,n}$.

Let $V(\mathcal{R}_{g,n})$ be the set of all pant decompositions of $\Sigma_{g,n}$, considered up to isotopy. We connect two vertices in $V(\mathcal{R}_{g,n})$ by an edge F if the corresponding decompositions are related to one another by an F move (where the F move is defined as in $\tilde{\mathcal{R}}_{g,n}$, just forgetting about the ordering of the curves). Moreover, we insert an edge T_a between two vertices if the corresponding decompositions are related to one another by the Dehn twist along a simple closed curve a . To the 1-dimensional complex obtained above, we add 2-cells of *combinatorial* type (bigons, triangles, squares and pentagons of F moves), *topological* type (braids, lanterns, chains, squares of T moves and one sided 2-cells corresponding to twists along the curves of a decomposition) and *mixed* type (triangles as in Figure 31, squares $FT_a = T_a F$). We remark that bigons and pentagons change their shape when passing from the decorated setting to the non-decorated one (as depicted in Figure 34), while all the other cells maintain the shape of the corresponding ones of $\tilde{\mathcal{R}}_{g,n}$.

We define $\mathcal{R}_{g,n}$ to be the complex having $V(\mathcal{R}_{g,n})$ as the set of vertices, edges and 2-cells as above. The two maps $t_{g,n} : \tilde{\mathcal{R}}_{g,n} \rightarrow \mathcal{R}_{g,n}$ (which forgets about the ordering of the curves) and $p_{g,n} : \mathcal{R}_{g,n} \rightarrow \mathcal{S}_{g,n}$ (which forgets about the topological information, keeping track of the combinatorial one only) are well defined. Moreover, it is easy to show that $p \circ t = s \circ r$. We may now state our core result.

Theorem 12. *The complex $\mathcal{R}_{g,n}$ is simply connected.*

Proof. Let γ be a loop in $\mathcal{R}_{g,n}$, based at the decomposition D . Hence γ is a sequence of F moves and Dehn twists, transforming the decomposition D into itself. We choose a decorated pant decomposition $D_1 \in t_{g,n}^{-1}(D)$ and we lift the loop γ edge

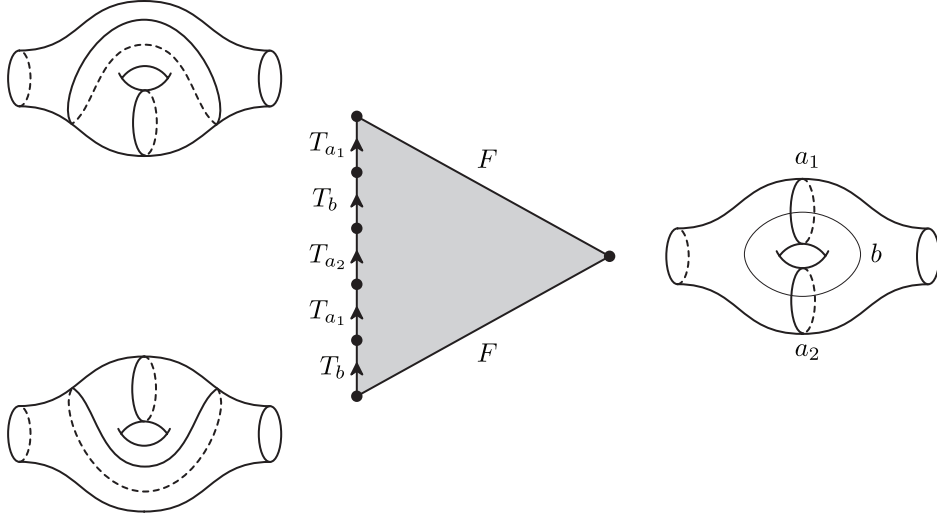


FIGURE 34. A bigon of pant decompositions.

after edge, starting from D_1 . We get in this way a path $\tilde{\gamma}$ in $\tilde{\mathcal{R}}_{g,n}$, whose second end is a decomposition D_2 , still belonging to $t_{g,n}^{-1}(D)$. The curves in D_1 and D_2 are identical, possibly except for their enumeration. Hence there exists a path of τ moves connecting D_2 to D_1 in $t_{g,n}^{-1}(D)$. Such path allows us to close the path $\tilde{\gamma}$ to a loop, based at D_1 , which will be denoted by $\tilde{\gamma}$. As $\tilde{\mathcal{R}}_{g,n}$ is simply connected, $\tilde{\gamma}$ is contractible, i.e. it may be homotoped to a point by means of the 2-cells of $\tilde{\mathcal{R}}_{g,n}$. Projecting the loop $\tilde{\gamma}$ and the homotopy in $\mathcal{R}_{g,n}$ with the map t , we get that the loop $\gamma = t(\tilde{\gamma})$ is contractible as well, thus proving the Theorem. \square

Remark 13. The topological cells provided by the Dehn style presentation are supported in subsurfaces homeomorphic to sporadic surfaces, living at the first and second Grothendieck floor (i.e. such that $3g - 3 + n = 1, 2$). The same is true for all the other cells of $\mathcal{R}_{g,n}$. Hence, $\mathcal{R}_{g,n}$ turns out to have a presentation with generators and relations supported in sporadic surfaces, illustrating in this way the simplified version of the Grothendieck conjecture recalled in the introduction.

REFERENCES

1. B. Bakalov and A. Kirillov Jr., *Lectures on tensor categories and modular functors*, University Lecture Series, no. 21, AMS, 2001.
2. B. Bakalov and A. Kirillov, *On the Lego-Teichmüller game*, Transform. Groups **5** (2000), 207–244.
3. A. Beilinson, B. Feigin, B. Mazur, and A. Polishchuk, *Introduction to rational field theory on algebraic curves*.
4. S. Benvenuti, *Finite presentations for the mapping class group via the ordered complex of curves*, Adv. Geom **1** (2001), 291–321.
5. J. Birman, *Braids, links, and mapping class groups*, Ann. of Math. Studies, no. 82, Princeton Univ. Press, 1975.
6. L. Funar and R. Gelca, *On the groupoid of transformations of rigid structures on surfaces*, J. Math. Sci. Univ. Tokyo **6** (1999), 599–646.
7. S. Gervais, *Presentation and central extensions of mapping class groups*, Trans. Amer. Math. Soc. **348** (1996), 3097–3132.
8. S. Gervais, *A finite presentation of the mapping class group of an oriented surface*, Topology **40** (2001), 703–725.
9. A. Grothendieck, *Esquisse d'un programme*, published in [13] (1984).
10. A. Hatcher, P. Lochak, and L. Schneps, *On the Teichmüller tower of mapping class groups*, J. Reine Angew. Math. **521** (2000).

11. A. Hatcher and W. Thurston, *A presentation for the mapping class group of a closed orientable surface*, *Topology* **19** (1980), 221–237.
12. C. Labruère and L. Paris, *Presentation for the punctured mapping class groups in terms of Artin groups*, *Algebr. Geom. Topol.* **1** (2001), 73–114.
13. P. Lochak and L. Schneps eds, *Geometric Galois actions, 1. Around Grothendieck “Esquisse d’un programme”*, London Math. Soc. Lect. Note Series, vol. 242.
14. M. Matsumoto, *A presentation of mapping class groups in terms of Artin groups and geometric monodromy of singularities*, *Math. Ann.* **316** (2000), no. 3, 401–418.
15. J. McCool, *Some finitely presented subgroups of the automorphism group of a free group*, *J. Algebra* **35** (1975), 205–213.
16. G. Moore and N. Seiberg, *Classical and quantum field theory*, *Commun. Math. Phys* **123** (1989), 177–254.
17. K. Walker, *On Witten’s 3-manifold invariants*, preprint (1991).

(Silvia Benvenuti and Riccardo Piergallini) DIPARTIMENTO DI MATEMATICA E INFORMATICA –
 UNIVERSITÀ DI CAMERINO, VIA MADONNA DELLE CARCERI 9, 62032 CAMERINO – ITALIA
E-mail address, S. Benvenuti: `silvia.benvenuti@unicam.it`
E-mail address, R. Piergallini: `riccardo.piergallini@unicam.it`